Journal of Non-Crystalline Solids 72 (1985) 369–389
North-Holland, Amsterdam

SOL → GEL → GLASS: III. VISCOUS SINTERING

George W. SCHERER

R&D Division, Corning Glass Works, Corning, NY 14831, USA

C. Jeffrey BRINKER and E. Peter ROTH

Sandia National Laboratories, Albuquerque, NM 87185, USA

Received 25 July 1984

Analysis of isothermal sintering data reveals that the viscosity of a gel increases with time. If the experiment is continued long enough, a limiting value of viscosity, η (final), is reached at each temperature. The increase in viscosity is attributed to two concurrent processes: condensation of hydroxyl groups and structural relaxation. Analysis of heat capacity (C_p) data permits an estimate of the viscosity (η) of the sintered glass. The results are in good agreement with η (final) from the sintering data. The approximate dependence of viscosity on hydroxyl content ([OH]) was established using η obtained from C_p data and [OH] from IR transmission spectra. The results indicate that structural relaxation contributes significantly to the rise in η during sintering.

1. Introduction

The densification of gels is a complex process. As revealed by constant heating rate shrinkage experiments [1], at least four mechanisms contribute to gel shrinkage: (1) capillary contraction; (2) condensation; (3) structural relaxation; and (4) viscous sintering. For the borosilicate composition used in this study, three temperature regions were identified coresponding approximately to: (I) weight loss with negligible shrinkage (25–150°C); (II) shrinkage and weight loss (150–525°C); and (III) dramatic shrinkage with little weight loss (525–700°C). Capillary contraction is the predominant shrinkage mechanism in Region I. Shrinkage in Region II results from skeletal densification which occurs primarily by condensation reactions accompanying the loss of water and organic residues. However (depending on the heating rate), a decrease in the rate of weight loss and a densification process with a different activation energy appear in the temperature interval 400–525°C. This shrinkage is attributed primarily to structural relaxation, i.e., the approach of the structure toward the configuration characteristic of the metastable liquid. Structural relaxation is achieved by diffusive motions of the atoms, without expulsion of water or other species. The boundary between Regions II and III is near the glass transition temperature, T_g, of the melted glass. The rapid shrinkage in Region III is the result of viscous flow which permits the tiny pores in the gel

0022-3093/85/$03.30

to collapse. The boundaries between these three regions are not well defined. In particular, condensation of hydroxyls and structural relaxation both may occur during viscous sintering, and have an important influence on the rate of shrinkage.

In this paper we present data on the rate of densification in Region III. By analyzing these measurements in terms of established models for viscous sintering, we can determine the flow behavior of the gel. Complementary structural studies, using the BET method, confirm the applicability of the sintering model.

In section 2, we review models of viscous sintering and choose the one most appropriate for our gel. Structural information obtained by nitrogen adsorption and electron microscopy is presented in section 3. Isothermal shrinkage data are analyzed in section 4 in terms of the viscous sintering model; the results indicate that the viscosity of the gel rises as sintering proceeds. A method for obtaining an estimate of viscosity from measurements of heat capacity is discussed in section 5. The results are compared with values found from the sintering data and shown to be in agreement. Explanations for the rise in viscosity during sintering are offered in terms of water loss, in section 6, and structural relaxation, in section 7. Conclusions are summarized in section 8.

2. Sintering models

Frenkel [2] laid the foundation for all subsequent analyses of viscous sintering. He pointed out that energy is dissipated as heat during viscous flow, and suggested that the reduction of surface area provides the source of this energy during viscous sintering. By equating these quantities, he derived a simple expression for the rate of coalescence of two spheres; a numerical error in his solution was corrected by Eshelby [3]. Frenkel's result, which predicts linear shrinkage proportional to time, is limited to the early stages of sintering, because of the geometric assumptions upon which it is based. Experimental studies [4,5] have verified Frenkel's prediction of the time dependence of sintering, and the underlying physical principles are considered to be well established. Of course, the sintering rate depends on the microstructure of the body, and this changes during the course of sintering. In the last stages, the body will contain isolated spherical pores whose rate of collapse will depend on both the radius of the pore and the permeability of the gas in the pores through the glass. A model to describe this situation was developed by Mackenzie and Shuttleworth [6]. Their result is applicable for any initial value of porosity, but only for a body with closed pores. As shown in fig. 1, this model predicts a sigmoidal variation of density with time. The dimensionless time variable is $\gamma n^{1/3} t/\eta$ where γ = surface energy, η = viscosity, t = time, and n = number of pores per unit volume of solid. For a given pore volume, the pore radius decreases as n increases. The rate of sintering increases as the pore

size and viscosity decrease, and as the surface tension increases. A model that describes the early and intermediate stages of sintering of a body with open pores was proposed by Scherer [7]. It was shown [8,9] to describe the densification kinetics of silica gels, porous VYCOR™, and soot bodies made by flame oxidation of $SiCl_4$. This model assumes that the microstructure is as shown in fig. 2: the solid phase is in the form of cylinders intersecting in a cubic array. To reduce their surface area, the cylinders tend to become shorter and thicker; when neighboring parallel cylinders touch, pores are isolated and thereafter the Mackenzie–Shuttleworth model applies. Fig. 1 reveals that the densification kinetics predicted for this model are very close to those predicted by Mackenzie–Shuttleworth when the relative density is $\geqslant 0.2$. This is a surprising, but very convenient, result: the sintering kinetics are weakly dependent on the microstructural model chosen. The virtue of the cylindrical array model is that the structure retains its form during densification. Frenkel's spheres lose their sphericity almost immediately, so the sintering kinetics must deviate from his prediction at an early stage. The cylindrical array changes only in scale, so it applies to both the initial and intermediate stages of sintering. The cylinder model predicts densification kinetics identical to Frenkel's model over the range of shrinkage to which Frenkel's model applies [10].

To compare the experimental sintering data to the theoretical models, one plots the time elapsed during an isothermal heat treatment against the dimensionless time corresponding to the density of the sample. The result should be a straight line with a slope of $\gamma n^{1/3}/\eta$, so that knowledge of two of these parameters permits determination of the third. The surface energies of several

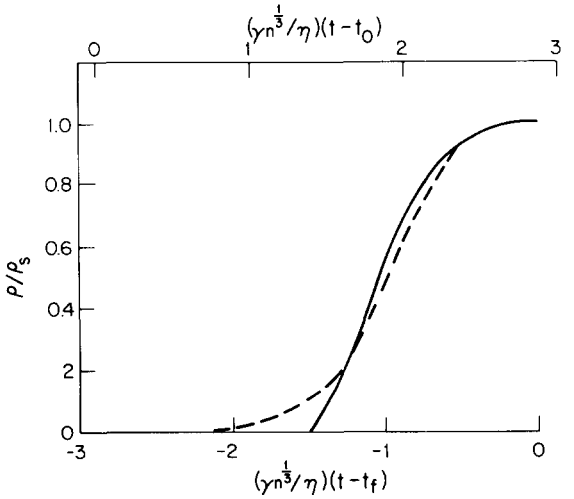

Fig. 1. Relative density vs Reduced time, for Mackenzie–Shuttleworth model, ref. [6] (———), and cylinder model, ref. [7] (— — —); t_f is the time at which $\rho/\rho_s = 1$; upper abscissa applies to cylinder model, where t_0 is the time when $\rho/\rho_s = 0$.

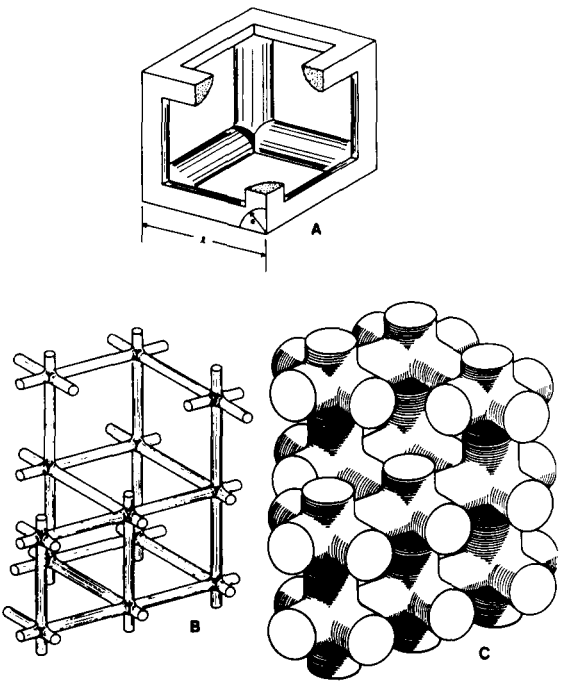

Fig. 2. Microstructural model consisting of cylinders in cubic array: A. Unit cell showing edge length, l, and cylinder radius, a; B. Model of low density microstructure ($\rho/\rho_s \approx 0.05$); C. Model of microstructure with $\rho/\rho_s = 0.50$.

glasses have been determined, and they range over about a factor of ~ 4, from ~ 80 erg/cm^2 for B_2O_3 [11] to ~ 315 erg/cm^2 for soda lime silica glass [12]. For the cylindrical array model [7], n can be determined by measuring the bulk density and the pore size (e.g. by gas adsorption–desorption analyses) or the surface area (by the BET method). The "unit cell" of the model structure is shown in fig. 2A. The cylinder radius is a and the distance between the centerlines of neighboring cylinders is l; the density is a function of $x \equiv a/l$:

$$\rho/\rho_s = 3\pi x^2(1 - cx), \tag{1}$$

where ρ = bulk density, ρ_s = density of the solid phase (i.e. skeletal density), and $c = 8\sqrt{2}/3\pi = 1.200$. The specific surface area is

$$S = \left(\frac{1}{l\rho_s}\right)\frac{2 - 3cx}{x(1 - cx)} \tag{2}$$

and the mean pore diameter may be approximated by

$$d = (2l/\sqrt{\pi})(1 - 2x). \tag{3}$$

Since one pore is trapped in each cell in the late stage of sintering, we find that [7]

$$n^{1/3} = \left(\frac{1}{l_0}\right)\left(\frac{\rho_s}{\rho_0}\right)^{1/3}, \tag{4}$$

where l_0 and ρ_0 are the respective initial values. In this paper, we compare the sintering kinetics of a gel with the cylindrical array model, for several reasons. First, it is the only available analysis of early and intermediate stage viscous sintering of an open-pore structure; second, as mentioned above, the sintering kinetics are not particularly model-sensitive, so we cannot be led far astray; finally, the model is consistent with the microstructural features discussed in Part I [13]. Using values of d and S found from nitrogen adsorption/desorption analyses, together with a reasonable estimate of γ, η is found by comparing the shrinkage data with the model.

3. Gel structure

To determine the structural parameters used in the sintering model, we have measured nitrogen adsorption and desorption isotherms. A typical pore size distribution for a gel heated to 525°C has a sharp peak near a radius of 10–12 Å. Electron microscopy reveals a very fine interconnected structure, similar to that shown in Part I [13] for a gel heated to 150°C. Table 1 shows the change in surface area, pore size, and density during isothermal treatments at 525° and 600°C, after heating to temperature at 2°C/min. At 525°C, the gel has an initial surface area of 412 m^2/g and bulk density of 1.30 g/cm^3; the density of a melted glass of the same composition is $\rho_s = 2.27$ g/cm^3, so $\rho/\rho_s = 0.57$. For this sample, eq. (1) gives $x = 0.31$, so eq. (2) implies $l = 48$ Å, and eq. (3) gives $d = 21$ Å, which compares well with the value $d = 17$–24 Å measured directly. Since the amount of the solid phase in the unit cell is constant, the bulk density is simply proportional to the volume of the cell, so

$$l/l_0 = (\rho_0/\rho)^{1/3}. \tag{5}$$

We should therefore be able to predict the change in surface area during sintering given the change in density, using eqs. (1), (2) and (5). As shown in table 1, the predicted values are in reasonable agreement with measured areas for the samples held at 600°C. (The sample held at 600°C for 21 h has reached a density at which the pores are becoming isolated, so the remaining surface is inaccessible to nitrogen, and the predicted value provides an upper bound for the measurable surface area.) However, the samples held at 525°C show a substantial loss of surface area with no commensurate increase in density. This suggests that a separate process, with an activation energy smaller than that of the viscosity, is operating at low temperatures. For example, the heavily hydrated surface layer may have much greater mobility than the solid phase as a whole, and may flow to fill in regions of high curvature such as surface roughness or necks between particles. This could reduce the surface area without causing shrinkage. As temperature increases, the viscosity drops rapidly and the rate of viscous sintering would produce more rapid changes in surface area than the mobile surface layer could. If this explanation is correct, one would expect the surface area to plateau eventually at 525°C as surface

Table 1
BET results

Heat treatment	BET			ρ (g/cm^3)	$P = \frac{1}{\rho} - \frac{1}{\rho_s}$ [a] (cm^3/g)	S(calc) [b] (m^2/g)
	Surface area (m^2/g)	Pore radius (Å)	Pore volume (cm^3/g)			
525°C No hold	412	8.5–11.5	0.315	1.30	0.329	(412 assumed)
525°C 15 min	342	11.5	0.328	1.315	0.319	
525°C 30 min	329	10–12	0.301	1.331	0.311	
525°C 2 h	267	10–12	0.262	1.363	0.293	
525°C 7 h	245	11–12	0.254	1.39	0.279	
525°C 24 h	215	10–12	0.282	1.42	0.263	377
600°C No hold	312			1.50		344
600°C 2 h	228			1.86		241
600°C 21 h	61.4			~ 2.2		< 107

[a] Assuming $\rho_s = 2.27$ g/cm^3.
[b] Assuming $S = 412$ m^2/g at 525°C (no hold).

irregularities are eliminated. Heat treatments of longer duration must be made to clarify this point.

A given volume of gel contains a certain volume of pores open to the atmosphere, V_P, and of solid phase, V_s, so the specific pore volume, P, is

$$P = V_P/\rho_s V_s \tag{6}$$

and the bulk density is

$$\rho = \rho_s V_s/(V_P + V_s). \tag{7}$$

Using eq. (7), we may rewrite eq. (6) as

$$P = \frac{1}{\rho} - \frac{1}{\rho_s}. \tag{8}$$

The good agreement shown in table 1 between the value of P calculated from eq. (8), with $\rho_s = 2.27$ g/cm^3, and that measured by N_2 adsorption indicates that closed pores are rare or absent in gels heated at or above ~ 525°C.

These measurements show that the microstructure of the gel is reasonably compatible with the model structure. The initial surface area and pore diameter at 525°C are consistent, and the change in S with ρ at 600°C follows

expectations. The rapid loss of surface area at 525°C is not satisfactorily understood. Small scale surface smoothing could decrease surface area without reducing the driving force for sintering. Alternatively, the drop in S without change in ρ could be interpreted as an increase in l_0 (see eq. (2)). If we were to analyze the sintering data in terms of the value of l_0 corresponding to the initial surface area (412 m^2/g), the change in l_0 would cause a change in the apparent viscosity, so that η would drift upward by as much as a factor of 2 over 24 h at 525°C. It should be noted, however, that no increase in l_0 (i.e. pore diameter) is observed.

Measurements of pore volume shed light on the densification processes occurring in Region II, particularly between 400 and 500°C. Using the measured pore volume and bulk density, we find [1], using eq. (8), that the density of the solid phase increases substantially in that temperature range with little associated weight loss. The data were interpreted to mean that the degree of cross-linking in the oxide network in the gel is much less than in a melted glass. Under these circumstances, the driving force for structural rearrangement is so great that densification of the network proceeds well below the glass transition temperature. Similar behavior is observed in glass cooled rapidly from the melt [14], but in that case the density change is 1–2 orders of magnitude smaller than in the gel. It is interesting to note that comparison of the pore volume and bulk density data would indicate a low value of ρ_s if closed pores were present. However, if the Region II densification is interpreted as viscous sintering of closed pores, they must be at least 10 times smaller than the open pores, because the latter do not shrink in Region II. Since the open pores are ~ 20 Å in diameter, the closed pores must have diameters on the order of the interatomic spacing; therefore, there is no meaningful distinction between such a "pore" and excess free volume in the network.

When structural relaxation occurs, all of the properties of the glass, including density and viscosity, change with time [14]. In most materials, viscous sintering occurs at such a low viscosity that relaxation is virtually instantaneous and no time dependence in η can be observed. However, the pores in alkoxide-derived gels are so small that sintering begins at $\sim 10^{13}$ P, so some structural relaxation may be occurring simultaneously. The effect would be an increase in viscosity with time; this point will be discussed in detail in sections 5 and 7.

4. Isothermal sintering

The sintering kinetics of the gels were measured using a dilatometer. Samples were heated in air at 1 or 2°C/min to the hold temperature and shrinkage was monitored as a function of time. Density changes were calculated using the shrinkage data together with weight loss measurements from companion runs using thermogravimetric analysis (TGA). The uncertainty in the densities so determined is estimated to be less than 5%. Fig. 3 shows results

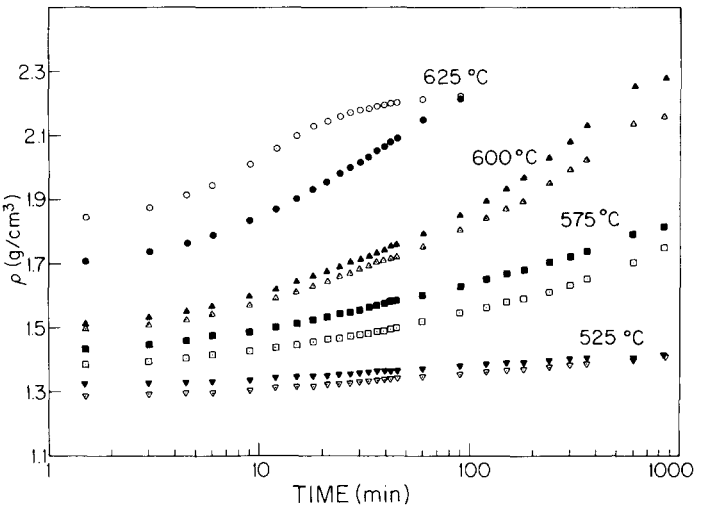

Fig. 3. Density versus time during isothermal holds at indicated temperatures; open and solid symbols represent replicate experiments.

for samples heated at 2°C/min; duplicate runs are in reasonable agreement.

To analyze the sintering during an isothermal hold in terms of the cylinder model, we use fig. 1 to find the dimensionless time corresponding to the density of each sample, then plot the dimensionless time against the hold time. The result should be a straight line with a slope equal to $K = (\gamma/\eta l_0)(\rho_s/\rho_0)^{1/3}$.

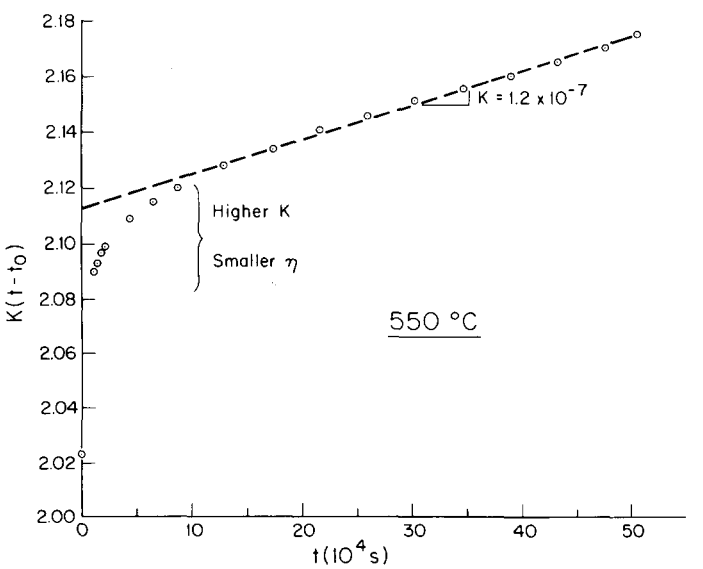

Fig. 4. Reduced time (from upper abscissa in fig. 1) versus elapsed time for isothermal hold at 550°C; decreasing slope indicates increasing viscosity.

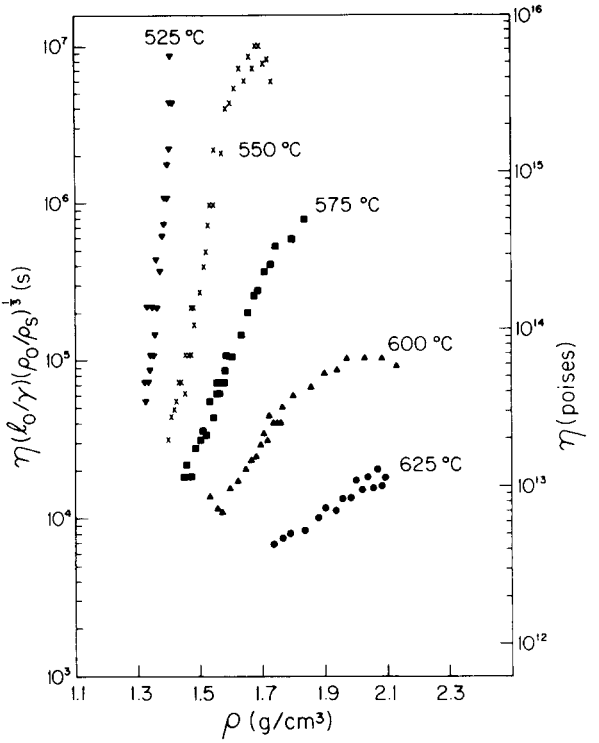

Fig. 5. Fitting parameter ($1/K$) from sintering data versus density for isothermal holds at indicated temperatures; data correspond to solid symbols in fig. 3; right ordinate is viscosity, calculated assuming $\gamma = 250$ erg/cm^2, $l_0 = 4.8$ nm.

Plotting the data from fig. 3 in this way, we find instead a curve of decreasing slope, as shown in fig. 4. To examine this behavior in detail, we fit the points pairwise to the model to obtain K for each succeeding pair of points. Fig. 5 shows the reciprocal of K, a quantity proportional to the viscosity, determined in this way. The viscosity seems to increase by ~ 200 times during the hold at 525°C, and by ~ 3 times at 625°C. Recall that the surface area decreases unexpectedly fast at 525°C, so the apparent value of l_0 would rise by a factor of ~ 2 with time. Neither that effect, nor the modest changes that might occur in γ upon volatilization of water or other glass components ($< 50\%$), can explain the observed change in K.

Several possible explanations could be offered for the lack of constancy of K. First, the shrinkage may not be caused by viscous sintering. However, compared to that in Region II, the weight loss in Region III is very small, so condensation reactions apparently do not contribute substantially to the shrinkage. Also, the pore volume data show that densification of the solid phase is essentially complete, so skeletal densification cannot cause the observed shrinkage. In fact, we know of no process other than viscous sintering that could produce significant shrinkage above 525°C. Second, the sintering

model could be inappropriate. This seems unlikely, since the sintering kinetics are weakly model-dependent and the BET results indicate a narrow distribution of pore diameters and no closed porosity. Therefore, we are led to the conclusion that the viscosity of the glass is rising as sintering proceeds. One obvious cause could be the loss of water from the gel during the isothermal hold. While the loss is far less than in Regions I or II, a small amount of water can have a dramatic influence on the viscosity [15]. The influence of water content on viscosity, and hence on sintering, will be examined in section 6. Another cause of a time-dependent viscosity could be structural relaxation. Although by 525°C the skeletal density has approached that of a melted glass, a very small change in density can be accompanied by a large change in viscosity. In section 7, we will discuss in detail the importance of structural relaxation during sintering.

The viscosity, η, can be found from K by using the parameters given in section 3 [$\rho_0/\rho_s = 0.57$ and $l_0 = 48 \times 10^{-8}$ cm] and an assumed value for γ. The surface energy for a molten glass is typically ~ 250 erg/cm^2, but that value is lowered by a large concentration of silanol groups [16]. We cannot quantify the latter effect for this glass, so we assume $\gamma = 250$ erg/cm^2 and obtain the results shown on the right ordinate in fig. 5. At 600°C, the viscosity increases to $\sim 7 \times 10^{13}$ P, then becomes constant; a similar, though less clearly defined, plateau appears at $\sim 10^{13}$ P at 625°C. In an attempt to find such a plateau at a lower temperature, a sample was held in the dilatometer at 550°C for 140 h. As shown in figs. 4 and 5, the viscosity becomes roughly constant at $\sim 6 \times 10^{15}$ P. The viscosities at these three plateaus are shown as η(final) in fig. 6; also shown are the initial viscosities for each sintering temperature. Note that sintering occurs at very high viscosities, because the tiny pores in the gel provide an enormous capillary force.

Fig. 7 shows the deviation of the present shrinkage data from the form predicted by Frenkel:

$$\log\left(\frac{\Delta l}{l}\right) = \log\left(\frac{3\gamma}{8r\eta}\right) + \log t. \tag{9}$$

At very short times, the slope is 1, as expected; then the rising viscosity causes downward curvature. The initial viscosity found from the linear regions, assuming $\gamma = 250$ erg/cm^2 and $r = 2.0$ nm, is shown in fig. 6, together with the initial viscosities from fig. 5. The results are nearly identical; the activation energy of ~ 30 kcal/mol. is much lower than expected for an oxide glass. Actually this apparent activation energy has no physical meaning, because the initial hydroxyl content, [OH], is different at each temperature. The high [OH] at 525°C reduces the viscosity at that temperature, bringing it closer to the value for the drier glass at 625°C. Consequently, the temperature dependence of η appears small. As we shall see in section 6, as sintering proceeds, [OH] approaches a similar value for samples fired at different temperatures. Therefore, the "final" viscosities, from the plateaus in fig. 5, show the much more reasonable activation energy of 122 kcal/mol.

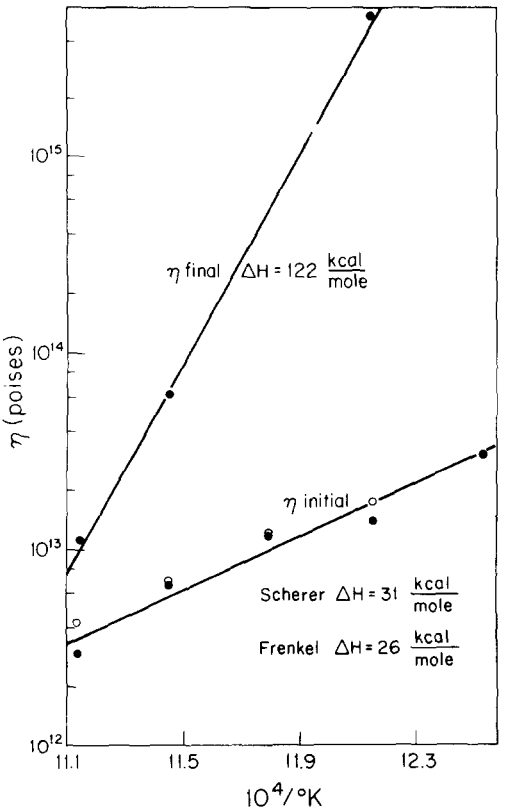

Fig. 6. Log (viscosity) versus $10^4/T(K)$ for data from plateaus in fig. 5 [η(final)] and from start of isothermal hold [η(initial)] based on cylinder [7] (●) and sphere [2] (○) models.

It has not been possible to compare the "final" viscosity values from the sintering data with direct viscosity measurements on gel-derived glass. However, it is possible to obtain an indirect test by analysis of enthalpy relaxation, as discussed in the next section.

5. Structural relaxation

The change in any glass property, p, such as volume, during continuous cooling is illustrated in fig. 8A. The slope of the curve, $\alpha_p \equiv dp/dt$, is higher in the liquid ($\alpha_p = \alpha_{pl}$) above the glass transition than in the rigid glass ($\alpha_p = \alpha_{pg}$). The reason is that there are two contributions to the temperature dependence of p:

$$\alpha_{pl} = \alpha_{ps} + \alpha_{pg}, \tag{10}$$

where α_{ps} results from structural rearrangements in the glass and α_{pg} depends only on temperature (the "vibrational" contribution). As the temperature

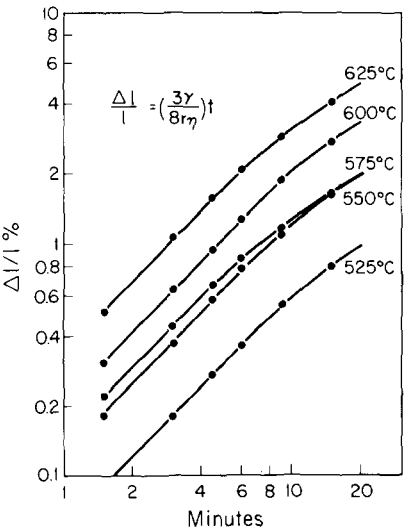

Fig. 7. Early stage isothermal shrinkage data; initial slope equals unity as predicted by Frenkel [2], but rising viscosity causes decrease in slope.

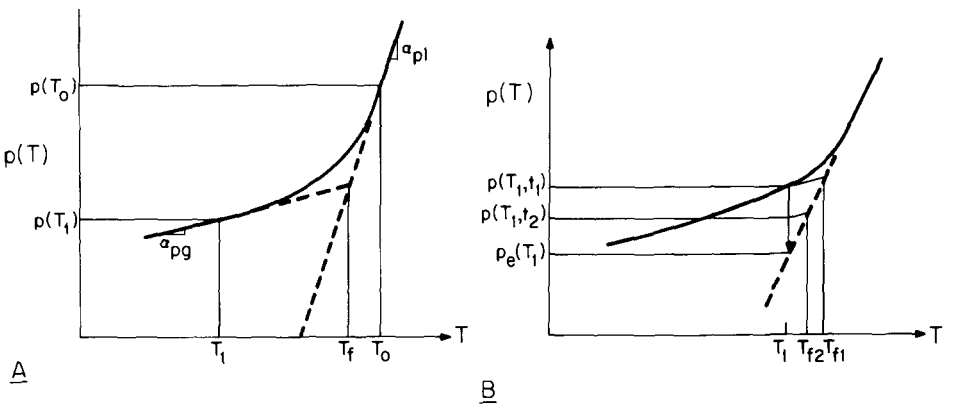

Fig. 8. Change in property p during cooling of glass-forming liquid: A. Slope decreases from α_{pl} to α_{pg} during transition from liquid to glass; when temperature is T_1, fictive temperature is T_f; B. Change in p during isothermal hold at T_1 following cooling to that temperature; T_f decreases with time from T_{f1} toward T_1 as p relaxes from $p(T_1, t_1)$ toward $p(T_1, \infty) = p_e(T_1)$, i.e. the equilibrium value at T_1.

decreases, structural changes become increasingly sluggish, so less of α_{ps} is observed: well below the glass transition, α_p is simply equal to α_{pg}. If the liquid were cooled infinitely slowly, p would follow the dashed extrapolation of the high temperature (i.e. the equilibrium) portion of the curve. The faster the cooling rate, the higher the temperature at which the property deviates from the equilibrium curve. The fictive temperature, T_f, is defined as the

intersection of the extrapolations of the liquid and glass portions of the curve. T_f provides a convenient, but incomplete, measure of the departure of the glass from its equilibrium condition. If the glass is annealed at temperature T_1, p will change with time toward its equilibrium value (i.e. the extrapolation of the liquid curve), as shown in Fig. 8B. At time t_2, the fictive temperature will have dropped to T_{f2}; relaxation (also called equilibration or stabilization) is complete when $T_f = T_1$ and p rests on the equilibrium curve.

The heat capacity is sensitive to the structure of a liquid, so it changes sharply during cooling through the glass transition region, as structural changes are arrested. The time- and temperature-dependence of the enthalpy, H, and isobaric heat capacity, $C_p = dH/dT$, can be analyzed using Narayanaswamy's model of structural relaxation [17]. The application of that model to DSC data has been developed extensively by Moynihan and his colleagues [18,19] and applied by Gonchukova [20] and Hodge and Berens [21]. Those workers have discussed the procedure in detail, so only a brief outline is presented here.

The temperature dependence of property p, illustrated in fig. 8, applies to the enthalpy, as well as to the volume and fluidity (i.e. reciprocal of viscosity). The slope of the equilibrium liquid curve, H_1, is $\alpha_{pl} = C_{pl}$, and the slope of the nonequilibrium (glass) curve is $\alpha_{pg} = C_{pg}$. The DSC measures the enthalpy, H, which may be written as [19]

$$H(T) = H_1(T_f) - \int_T^{T_f} C_{pg}\, dT', \tag{11}$$

where T_f is the fictive temperature for the enthalpy. The fictive temperature is given by [17]

$$T_f = T - \int_0^{\xi} M_H(\xi - \xi') \frac{dT}{d\xi'} d\xi' \tag{12}$$

where M_H is the relaxation function for H, and ξ is the reduced time defined by

$$\xi = \tau_{Hr} \int_0^t \frac{dt}{\tau_H(T, T_f)} = \tau_{Hr} \int_{T(0)}^{T(t)} \frac{dT'}{q\tau_H(T, T_f)}, \tag{13}$$

where $\tau_H(T, T_f)$ is the relaxation time for the enthalpy, $\tau_{Hr} = \tau_H(T_r, T_r)$, T_r is an arbitrarily chosen reference temperature (above the transition region), $T(t)$ is the temperature at time t, and $q = dT/dt$. The relaxation time is

$$\tau_H = \tau_0 \exp\left(\frac{x\Delta H}{RT} + \frac{(1-x)\Delta H}{RT_f} \right), \tag{14}$$

where τ_0 and x are constants ($0 \leqslant x \leqslant 1$), ΔH is an activation energy, and R is the ideal gas constant. It is generally observed [18–20] that $x \approx 0.4$–0.5, and that ΔH for τ_H is the same as for the viscosity:

$$\eta = \eta_0 \exp(\Delta H/RT). \tag{15}$$

The relaxation function is satisfactorily represented by [18–21]

$$M_H(\xi) = \exp\left[-(\xi/\tau_{Hr})^b \right] = \exp\left[-\left(\int_{T(0)}^{T(t)} \frac{dT'}{q\tau_H} \right)^b \right], \tag{16}$$

where b is a constant; typically, $b \approx 0.6$–0.8. This function is equivalent to a distribution of relaxation times which is broader when b is smaller [14].

For the calculations presented in this paper, we used $\Delta H = 122$ kal/mol, as determined from the sintering data. It should be noted that this value is based on η(final) for gels sintered at different temperatures, so that each may have a different hydroxyl content. If [OH] differs significantly with temperature, ΔH would not represent the temperature dependence of any one glass. Fortunately, our results indicate that the variation in the final [OH], if present, is small, as will be shown. To fit the DSC data, we used the formalism outlined above, assuming the typical value $x = \frac{1}{2}$, and adjusting τ_0 and b. More extensive heating and cooling data would be needed to establish all of the parameters with precision; a detailed study of that kind is planned. For the present, the available data are sufficient to provide an estimate of τ_0.

For the DSC study, gels were subjected to 4 different heat treatments: 525°C for 15 min, 2 h, and 24 h; 600°C for 17.75 h. These samples were heated in the DSC to 990 K to achieve complete sintering and structural relaxation. They were then cooled at 80 K/min and reheated at 10 K/min; the analysis was applied to the latter heating data. Calculations revealed that the data for the samples pre-treated at 525°C were fit well using $b = 0.5$, as shown in fig. 9. This is an uncommonly low value, corresponding to a broad distribution of relaxation times. The sample pretreated at 600°C was more accurately fit with $b = 0.4$ than 0.5; it is not clear whether this indicates a real difference in behavior, or merely the uncertainty in these preliminary data. Fig. 10 shows the curves corresponding to $b = 0.5$. It is important to note that the best value of τ_0 was hardly influenced by the value of b (3×10^{-28} versus 4×10^{-28} s).

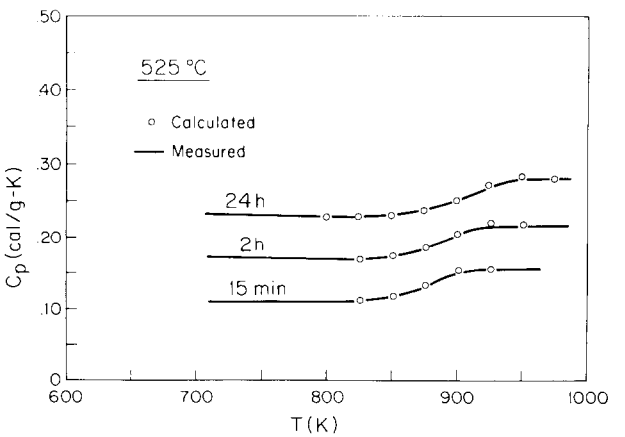

Fig. 9. Measured (———) and calculated (○) heat capacity during heating at 10 K/min for samples previously held at 525°C for indicated times, heated in DSC to 1000 K, then cooled at 80 K/min; ordinate correct for 24 h sample, others shifted downward by 0.05 and 0.10 cal/g K, respectively.

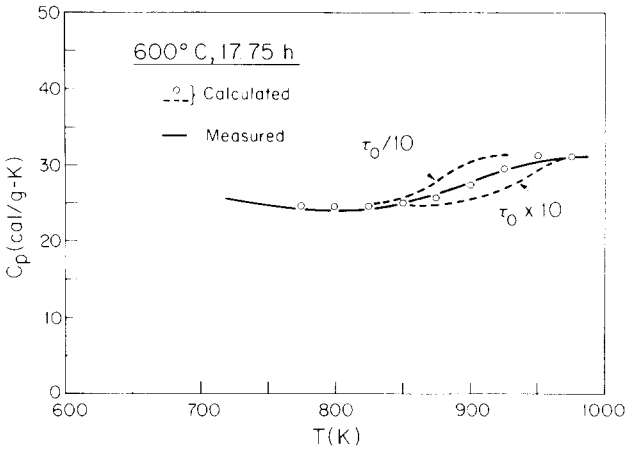

Fig. 10. Measured (———) and calculated (○) heat capacity during heating at 10 K/min for sample previously held at 600°C for 17.75 h, heated in DSC to 1000 K, then cooled at 80 K/min; dashed lines show results of calculations if relaxation time is change by a factor of 10.

Our results are in contrast to the results of Gottardi et al. [23], who observed a sharp glass transition (reflecting a narrow distribution of relaxation times) in a gel glass. The apparent discrepancy may have to do with the structural differences between our alkali borosilicate and their alkali borophosphate glass.

Since ΔH is the same for η and τ_H, they are proportional to each other:

$$K_H = \eta/\tau_H = \eta_0/\tau_0, \tag{17}$$

where K_H is a constant with the dimensions of an elastic modulus. Typically, for a multicomponent silicate glass [14,23],

$$\log_{10} K_H(\mathrm{dyn/cm^2}) \approx 10.2 \pm 0.3. \tag{18}$$

The values of η_0 in table 2 were found from the best-fit τ_0's, using $K_H = 2 \times$

Table 2
Hydroxyl content of sintered gels

Heat T(°C)	Treatment t(h)	Relative peak height (2.7 μm)	Hydroxyl [a] content (wt%)	T_g(°C) [b]	η_0(Poises) [c]
525	0	1.0	0.33		
	0.33	0.92	0.31	597	4.0×10^{-19}
	2.0	0.44	0.15	612	1.2×10^{-18}
	24.0	0.33	0.11	630	5.5×10^{-18}
600	17.75	0.21	0.07	634	7.0×10^{-18}

[a] Assuming extinction coefficient = 56 l/mol. cm.
[b] Glass transition temperature from DSC curves, defined as the temperature at which C_p is halfway between liquid and glass values.
[c] Values found from analysis of enthalpy relaxation.

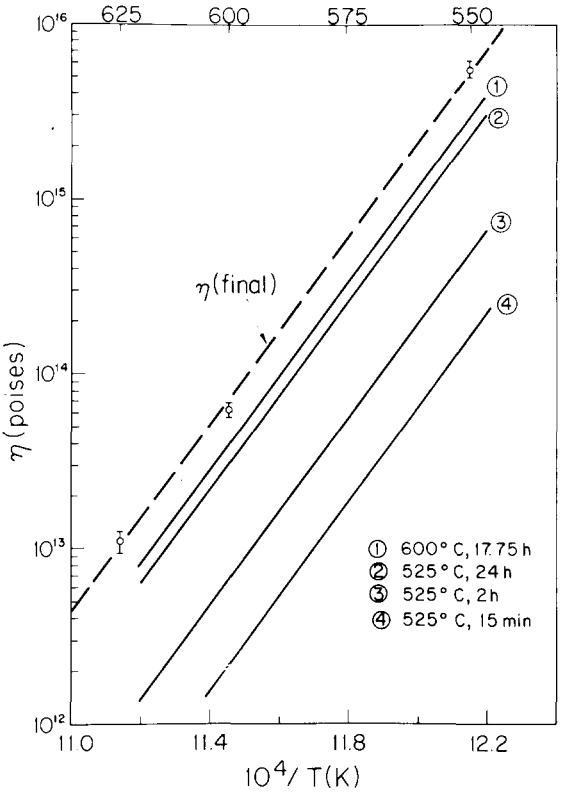

Fig. 11. Log (viscosity) versus $1/T$(K) from analysis of heat capacity data in figs. 9 and 10; symbols represent η(final) from sintering data from fig. 6.

10^{10} dyn/cm^2; the viscosities calculated from eq. (15) are shown in fig. 11. The close agreement for the samples pretreated for 17.75 h at 600°C and 24 h at 525°C suggests that the [OH] ultimately approaches the same value at different temperatures. Therefore, the activation energy of η(final) in fig. 6 should pertain to glass with [OH] $\approx$ 0.07–0.11 wt.%, as discussed in the next section. The close correspondence between η(final) and the viscosity values extracted from the DSC data shows that the plateaus in fig. 5 indeed represent the true viscosity of the glass. Changing η by an order of magnitude would shift the C_p curve as shown by the dashed lines in fig. 10, so we conclude that η(final) is well within a factor of 10 of the true viscosity of the glass.

6. Effect of hydroxyl on viscosity

In section 5 we determined the viscosity of densified gels using a structural relaxation model and made comparisons with values of "final" viscosities determined from the sintering model. In this section we attempt to establish

how viscosity varies with hydroxyl content in order to determine the contribution of dehydroxylation to the measured isothermal increases in viscosity.

It is well known [15] that hydroxyl ions reduce the viscosity of glass, but there are no quantitative data for any composition similar to that used in this study. However, we can use the temperature dependence of the heat capacity, C_p, to estimate the change in η with OH content, as discussed in the previous section. The symbols in fig. 9 show the C_p curves calculated by the method described in section 5. The relaxation times determined by fitting the calculations to the data correspond to the viscosities shown in fig. 11. The viscosity increases with time of treatment at 525°C; the viscosity curve for the sample held 24 h is about the same as for the sample held for 17.75 h at 600°C. Note that all of the DSC curves were analyzed assuming $\Delta H = 122$ kcal/mol, ignoring any influence of hydroxyl content, [OH], on the activation energy. It is not known how much error might result from that assumption, but the good fits to the C_p data suggest that it is not serious.

After removal from the DSC, the hydroxyl contents of the sintered gels were measured by infra-red spectroscopy. The extinction coefficient at 2.7 μm was assumed to be 56 l/mol. cm [24], a value that is expected to be within 20% of

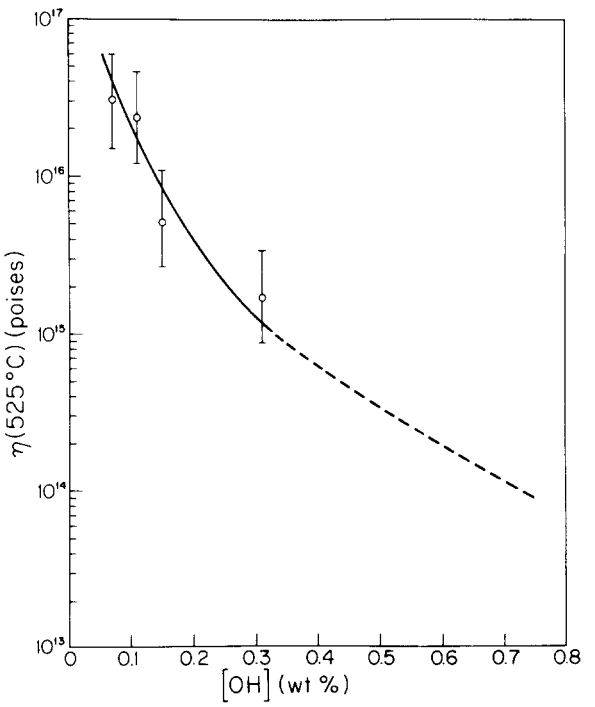

Fig. 12. Viscosity at 525°C versus hydroxyl content, based on η_0 found from heat capacity data (see table 2). Dashed line shows extrapolation over range of [OH] in gel during isothermal hold at 525°C from 15 min to 24 h.

the true value for the present composition [25]. The results are presented in table 2. Two other gel samples that had previously been held at 525°C for 15 min and 24 h, respectively, were reheated in the thermogravimetric analyzer (TGA) at the same heating rate used in the DSC. The weight loss was found to be 0.45 wt% for the gel held 15 min and 0.21 wt % for the gel held 24 h. The hydroxyl content of the gel at the end of the hold must equal the weight lost (from TGA) plus the OH retained (from IR absorption). Therefore, the gel must have contained 0.76 wt % OH after 15 min and 0.32 wt% OH after 24 h at 525°C.

Fig. 5 shows that the viscosity rose by a factor of ~ 160 during the isothermal hold of 14 h at 525°C. The change in hydroxyl content of the gel must have been less than the 0.44 wt% lost in the interval from 15 min to 24 h, but let us use that value as a generous upper bound. Fig. 12 shows η(525°C) versus [OH], using viscosity data from fig. 11 and the corresponding hydroxyl contents from table 2. Unfortunately, the data do not cover the range 0.32 wt% < [OH] < 0.76 wt% that applies to the sample during sintering. However, it is evident that any reasonable extrapolation of the data in fig. 12 will give a change in η no larger than a factor of ~ 20 over that range of [OH]. That means that a substantial fraction of the increase in η during sintering, perhaps as much as an order of magnitude, is not attributable to change in [OH]. As mentioned earlier, a factor of ~ 2 results from changes in the microstructure (loss of surface area). The rest of the increase, a factor of 5 or more, is probably caused by structural relaxation.

7. Effect of relaxation on viscosity

If the equilibrium viscosity of a glass is given by the Arrhenius equation, eq. (15), then the nonequilibrium viscosity can be approximated by [17]

$$\eta = \eta_0 \exp\left(\frac{x\Delta H}{RT} + \frac{(1-x)\Delta H}{RT_f} \right), \tag{19}$$

where x is a constant ($0 \leqslant x \leqslant 1$). The estimates presented in section 6 suggest that structural relaxation may cause a significant fraction of the viscosity increase at 525°C, although the changing hydroxyl content is probably the dominant factor. Relaxation will cause smaller changes during isothermal holds at higher temperatures, as relaxation will occur during heating to the hold temperature. However, hydroxyl loss will also be less at higher temperatures, so both effects may still be important.

For an ordinary window glass quenched into a salt bath, T_f may be ~ 65°C higher, and the density ~ 0.4% lower, than in the same glass cooled at ~ 1°C/min [26]. If the quenched glass is annealed to eliminate that density difference, the viscosity will rise by a factor of ~ 25. The densification of the gel in Region II is enormously greater than that in a quenched glass [1]. Although the measured skeletal density is nearly the same as for the melt-formed

glass, it seems probable that some excess volume is still present at the beginning of Region III, so that a small densification and substantial rise in viscosity could occur simultaneously with sintering.

As we have said, structural relaxation occurs for all glass properties including enthalpy as well as volume and viscosity. Therefore if structural relaxation contributes to gel densification in Region III, we should be able to observe it by DSC. Unfortunately, three additional processes: sintering, polymerization, and vaporization of water (a by-product of polymerization) occur concurrently and strongly influence the DSC results. As Frenkel [2] pointed out, the surface area recovered during sintering is dissipated as heat as the glass flows. Consequently, we expect an exothermal equal to the product of the surface energy times the change in surface area. Additionally, as discussed in Part II [1], polymerization is normally assumed to be weakly exothermic [16] while vaporization of water is strongly endothermic (0.5 kcal/g).

DSC of a sample originally quenched from 525°C after a twenty minute isothermal hold shows only a weak exotherm (-4.0 cal/g) while the exotherm expected from sintering equals -21 cal/g (330×10^4 cm^2/g $\times$ 250 erg/cm^2). Obviously the sintering exotherm is almost completely obscured by the heats associated with polymerization and vaporization. Thus it is likely that the relatively weak exotherm expected due to structural relaxation would be equally obscured so that, in this case, it is not possible to prove unambiguously the existence of structural relaxation by DSC.

The difference between the measured exotherm and that expected from sintering ($+17$ cal/g) is attributable to polymerization and vaporization. According to Dzis'ko et al. [27] the hydroxyl group retention at 525°C for a gel of 20 Å average pore diameter is estimated to be ~ 5 OH/nm^2, requiring 13 cal/g for vaporization (assuming $S = 330 \times 10^4$ cm^2/g and ΔH vaporization $= 0.5$ kcal/g). The 4 cal/g that remains unaccounted for suggests that we overestimated the surface energy (silanols reduce the surface energy of the gel; if we assume $\gamma < 250$ erg/cm^2, we require a correspondingly smaller endotherm to balance the heats) or that the polymerization process is not weakly exothermic but instead endothermic, on average, as discussed in Part II [1].

Isothermal holds at 525°C reduce the surface area (table 1), but cause the DSC exotherm to increase. Thus the decrease in recovered surface energy is more than compensated for by increased amounts of polymerization and vaporization during the isothermal hold (reduced amounts of polymerization and vaporization during the DSC experiment). Unfortunately increased isothermal holds will also reduce the excess free volume so that, although the magnitude of the masking endotherm is reduced, the magnitude of the exotherm expected from structural relaxation is likewise reduced.

We cannot demonstrate the occurrence of structural relaxation using the DSC, because the exotherm (if it exists) is obscured by the vaporization endotherm. Since water loss and structural relaxation both cause the viscosity to rise, we cannot unambiguously ascribe the viscosity increase to one effect or the other. It seems highly likely that both contribute, but no quantitative

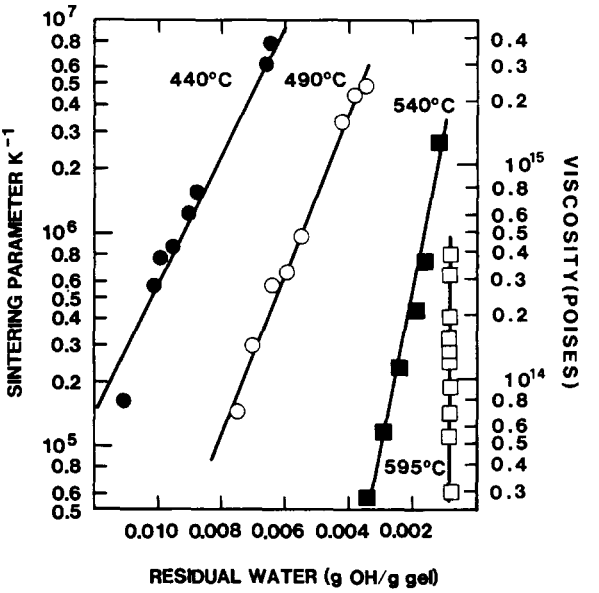

Fig. 13. Sintering parameter K^{-1} (and viscosity) vs. [OH] during 18 h isothermal treatments; from Gallo et al. [28].

attribution is possible. Nevertheless, the dramatic relaxation in Region II [1] suggests that excess volume (high T_f) is present at the onset of Region III, and the relaxation of that excess volume could be responsible for much of the rise in η in the sintering experiments.

The importance of structural relaxation is supported by recent work on a gel similar to that studied here. Using TGA and IR spectroscopy, Gallo et al. [28] determined the water content of the gel during sintering. The data for different temperatures seem to converge as [OH] decreases, which would imply that the activation energy for viscous flow decreases. However, it is generally observed that the activation energy decreases as the hydroxyl content *increases*. The apparent contradiction is resolved by consideration of the effect of structural relaxation, which causes η to increase with no change in hydroxyl content, and thereby increases the slopes of the lines in fig. 13. The slope of the line corresponding to 440°C is dominated by the change in [OH] and the slopes for higher temperatures are increasingly influenced by structural relaxation. The large increase in η at 595°C occurs with no detectable change in [OH], and must be attributed entirely to structural relaxation.

8. Conclusions

The isothermal sintering of the investigated alkoxide-derived gel is accompanied by a substantial increase in viscosity with time. Some of that increase is

caused by the continual loss of water. The effect of hydroxyl content on viscosity is revealed by the shift of the glass transition temperature observed in the DSC. That effect can be quantified by applying the phenomenological theory of structural relaxation proposed by Narayanaswamy. The data suggest that much, but not all, of the increase in η during sintering results from the decrease in [OH]. Structural relaxation probably accounts for the remaining portion of the rise in η. The volume relaxation needed to achieve that effect would be a tiny fraction of the relaxation that is observed in Region II. A more detailed study of enthalpy relaxation is planned, which will expand our knowledge of the dependence of η on [OH]. This will permit a better estimate of the importance of structural relaxation during sintering.

References

[1] C.J. Brinker and G.W. Scherer, J. Non-Crystalline Solids 70 (1985) 301.
[2] J. Frenkel, J. Phys. (Moscow) 9 [5] (1945) 385.
[3] J.D. Eshelby, Trans. AIME 185 [11] (1949) 806.
[4] G.C. Kuczynski, J. Appl. Phys. 20 (1949) 1160.
[5] W.D. Kingery and M. Berg, J. Appl. Phys. 26 [10] (1955) 1205.
[6] J.K. Mackenzie and R. Shuttleworth, Proc. Phys. Soc. London 62 [12B] (1949) 833.
[7] G.W. Scherer, J. Am. Ceram. Soc. 60 [5–6] (1977) 236.
[8] G.W. Scherer and D.L. Bachman, J. Am. Ceram. Soc. 60 [5–6] (1977) 240.
[9] G.W. Scherer and J.C. Luong, Proc. 2nd Int. Workshop, Glasses and Ceramics from Gels, Wurzberg, 1983, J. Non-Crystalline Solids 63 (1984) 163.
[10] G.W. Scherer, J. Am. Ceram. Soc. 67 (1984) 709.
[11] W.D. Kingery, J. Am. Ceram. Soc. 42 [1] (1959) 6.
[12] N.M. Parikh, J. Am. Ceram. Soc. 41 [1] (1958) 18.
[13] C.J. Brinker and G.W. Scherer, J. Non-Crystalline Solids 70 (1985) 301.
[14] O.V. Mazurin, J. Non-Crystalline Solids 25 (1977) 130.
[15] R.F. Bartholomew, in: Treatise on Materials Science and Technology, Vol. 22, Glass III, eds., M. Tomozawa and R.H. Doremus (Academic Press, New York, 1982).
[16] R.K. Iler, The Chemistry of Silica (Wiley, New York, 1979).
[17] O.S. Narayanaswamy, J. Am. Ceram. Soc. 54 [10] (1971) 491.
[18] C.T. Moynihan et al., N.Y. Acad. Sci. 279 (1976) 15.
[19] M.A. DeBolt et al., J. Am. Ceram. Soc. 59 [1–2] (1976) 16.
[20] N.O. Gonchukova, Sov. J. Glass Phys. Chem. 7 [3] (1981) 217 (English translation).
[21] I.M. Hodge and A.R. Berens, Macromolecules 15 (1982) 762.
[22] V. Gottardi, G. Scarinci and G. Carturan, Thermal Analysis, ed. H. Wiedemann (Birkhauser, Basel, 1980) p. 493.
[23] G.W. Scherer, J. Am. Ceram. Soc. 67 (1984) 504.
[24] J.P. Williams et al., Am. Ceram. Soc. Bull. 55 (1976) 524.
[25] H. Hoover, Corning Glass Works, private communication.
[26] M. Hara and S. Suetoshi, Reports Res. Lab. Asahi Glass Co. 5 [2] (1955) 126.
[27] V.A. Dzis'ko, A.A. Vishnevskaya and V.S. Chesalova, Zh. Fiz. Khim. 24 (1950) 1416.
[28] T.A. Gallo, C.J. Brinker, L.C. Klein and G.W. Scherer, in: Better Ceramics Through Chemistry, eds. C.J. Brinker, D.E. Clark, D.R. Ulrich (Elsevier–North-Holland, Amsterdam, 1984) p. 85.